Desalination and Water Treatment
www.deswater.com

doi: 10.5004/dwt.2017.1647

62 (2017) 192–199
February

Characteristics of metastable zone in the crystallization process: a case study of sparingly soluble hydroxyapatite

Hongliang Dai[a,b], Xiwu Lu[a,b,*], Yonghong Peng[a,b], Zixuan Yang[a,b], Huaqing Zhu[a,b]

[a]*School of Energy and Environment, Southeast University, No.2 Sipailou, Nanjing 210096, China, Tel. +86 025 83792614; Fax: +86 025 83792610; emails: daihongliang103@163.com (H. Dai), xiwulu@seu.edu.cn (X. Lu), pengyonghong809@126.com (Y. Peng), yzx_1009@sina.com (Z. Yang), zhqxl20@126.com (H. Zhu)*
[b]*ERC Taihu Lake Water Environment (Wuxi), No.99 Linghudadao, Wuxi 214135, China, Tel. +86 0510 85343801; Fax +86 0510 85343801*

Received 18 November 2015; Accepted 29 May 2016

ABSTRACT

Hydroxyapatite (HAP) crystallization for phosphorus recovery from wastewater is an economical and efficient approach. The metastable zone of solution is the precondition of crystallization process and is also the key to obtain high quality crystal products. HAP is a sparingly soluble salt, and the research on the metastable zone of HAP seems more complex than that of soluble salts. In this study, the characteristics of metastable zone of HAP crystallization at different saturation temperatures were studied by using the electrical conductivity and turbidity method. Effects of various experimental factors (crystal seeds, initial pH, stirring intensity, and impurity ions) on metastable zone width (MZW) were investigated. The results indicated that MZW was increased with the rise of cooling rate, and the presence of crystal seeds delayed the occurrence time of critical conductivity thus increasing the MZW. Calcite as the crystal seed exhibited the best performance on improving the MZW due to its specific surface area and composition among three tested seeds. MZW became narrow with the increase of the stirring intensity, and the acidic solution (pH 6.0) had a larger MZW than that in alkaline solution (pH 8.0). Several typical impurity ions could broaden the MZW of HAP, and the order of the impact on ΔMZW was: $CO_3^{2-} > Fe^{3+} > Cu^{2+} > SO_4^{2-}$.

Keywords: Metastable zone width; Hydroxyapatite; Induced crystallization; Phosphorus recovery; Crystal seeds

1. Introduction

Phosphorus is a limited and non-renewable mineral resource, making a major contribution to agricultural and industrial development [1, 2]. Excessive phosphorus content in wastewaters should be removed for controlling eutrophication and maintaining a sustainable environment for future generations [3]. With the increasing demand for phosphorus and the reducing available phosphorus resources, phosphorus recovery from wastewater has drawn more attentions [4]. To date, several traditional treatments have been widely investigated for phosphorus removal from domestic and urban wastewater, including chemical precipitation [5–7], biological [8, 9] and physical processes [10, 11]. However, many limitations hamper their applications, such as high cost, phosphorus source waste and secondary pollution. Induced crystallization for phosphorus recovery from the wastewater is an economical and efficient approach, possessing the characteristics of efficient phosphorus recovery and high quality crystallization products [12–14].

The metastable zone of solution is the precondition of crystallization process and is also the key to obtain high quality crystal products [15, 16]. The size distribution of crystal products tends to be more uniform, and the grain size is

* Corresponding author.

increased in metastable zone [17, 18]. The dependence of the experimentally measured metastable zone width (MZW), as determined by the maximum super-cooling $\Delta Tmax$ using the conventional poly-thermal method, of different solid solvent systems on various factors has been analyzed traditionally by using Nývlt's empirical equation [19]. Fig. 1 is a schematic illustration describing a typical metastable zone of crystallization process. It should be noted that industrial-scale batch crystallization operations have to follow the "Metastable Zone" for obtaining desirable crystal products (Fig. 1). Spontaneous nucleation is unlikely to occur within the metastable zone. The seeded crystallization process usually exhibited lower nucleation rate and better crystal size distribution (CSD) of products. Most solute molecules could be precipitated on the seed surfaces in solution while loading the crystal seeds [20]. Consequently, the presence of crystal seeds acts like a catalyst to reduce the activation energy barrier between the crystals and seeds.

To date, research on the removal or recovery of phosphorus for forming hydroxyapatite (HAP) from wastewater was mainly focused on the optimization of crystallization conditions [21, 22], the options of crystal seeds [23, 24] and the design of crystallization reactor [25, 26]. HAP is a sparingly soluble salt, and only few researches are focused on the crystallization mechanism of HAP due to the complicated measurement methods for trace concentration of HAP [27, 28]. Therefore, it is necessary to study the characteristics of MZW of sparingly soluble HAP in different experimental conditions for improving the efficiency of phosphorus recovery and the quality of crystallization products.

The aim of this study was to study the effects of various experimental factors on the MZW of HAP solution in a stirred tank crystallizer. First, a new method was developed to study the metastable region of sparingly soluble HAP in crystallization process. Subsequently, the optimization of crystal seeds and their dosage based on the variation amplitude of MZW were conducted. Finally, the initial pH, stirring intensity, and impurity ions were investigated for studying the impact on the MZW with the presence of crystal seeds. The results would illuminate the mechanism of sparingly soluble HAP in induced crystallization process and provide theoretical guidance for further study on the process optimization.

2. Materials and methods

2.1. Experimental apparatus

The induced crystallization of HAP in aqueous solutions was performed in a one liters lab-scale batch reactor (Fig. 2). Heating rate and cooling rate in the reaction system were controlled by digital thermostatic bath (8020 DC, Biosafer Co. Ltd., China). The solution conductivity was measured by conductivity meter (DDB-303A, Shanghai REX Instrument Factory, China) with instrumental resolutions ±0.1 μS/cm. The turbidity was monitored online using a turbidity meter (SOLITAX-1720E, HACH Co. Ltd., USA) with instrumental resolutions ±0.002 NTU. Agitation in the reactor was provided by a mechanical stirrer (JB500-D, Changzhou Guohua Co. Ltd., China) and stirring speed was ranged from 50 to 1,300 r/min.

2.2. The measurement of MZW of HAP crystallization

Metastable zone is a vital factor of nucleation kinetic [29–31], and the width of the metastable zone is dependent on various process parameters such as saturation concentration, presence of crystal seeds, impurity, cooling rate and agitation level [15, 17, 32]. In this study, MZW was measured for saturated solutions in seeded systems by using conductivity and turbidity technique. Batch tests were carried out by mixing a certain amount of HAP ($Ca_5(PO_4)_3OH$) (with an amount of 5 mmol) in a 1 L double jacketed stirred tank crystallizer with 700 mL of solution. The pH (7.0 ± 0.1) and conductivity (1,000 ± 100 μS/cm) were adjusted with NaOH and NaCl to be similar to the secondary treated effluent. The temperature of reaction system was controlled by thermostat. First, HAP was dissolved at a 200 r/min of stirring speed with 10°C/h heating rate at different temperatures (35, 40, 45, 50, 55, and 60°C), then filtering out the insoluble HAP using 0.45 μm filter at the same temperature. The filtered fluid was the saturated solution of sparingly soluble HAP at different saturated temperature (T_{sat}). Subsequently, the system was maintained

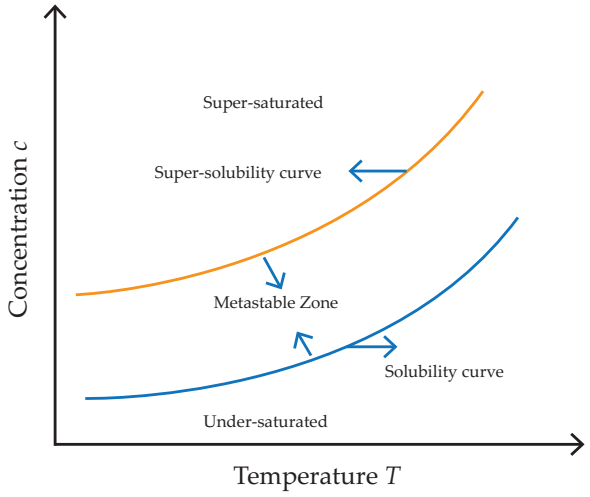

Fig. 1. Schematic illustration of a typical metastable zone of crystallization process.

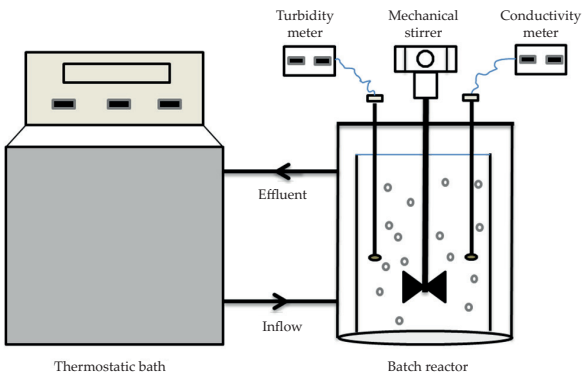

Fig. 2. Experimental apparatus of the batch reactor for HAP crystallization in aqueous solutions.

thermal insulation 30 min at the saturated temperature (T_{sat}) and then kept a constant cooling rate R of 5~25°C/h. The corresponding temperature (T_{lim}) was recorded when conductivity value abruptly decreased and turbidity value suddenly increased. The MZW is determined by poly-thermal method (Eq. (1)) [20]:

$$\mathrm{MZW} = \Delta T_{max} = T_{sat} - T_{lim} \quad (1)$$

2.3. Effects of various experimental factors on the MZW of HAP

Experiments were achieved at different pH 6.0, 7.0, 8.0 in a stirred reactor (1 L) filled with 700 mL solution with a rotational speed in the range of 100~500 r/min. Deionized water was used to prepare the synthetic wastewater solution. Three seeds (Quartzite, Calcite and Dolomite), seed dosage (1, 5, 20, 60 g/L), and four impurity ions (Fe^{3+}, Cu^{2+}, CO_3^{2-}, SO_4^{2-}) were conducted to study the variation of MZW. MZW variation was used to investigate the effects of crystal seeds dosage and impurity ions on the metastable zone of HAP induced crystallization, which was determined by Eq. (2):

$$\Delta\mathrm{MZW} = \Delta T_{max-imp} - \Delta T_{max} \quad (2)$$

In Eq. (2), $\Delta T_{max\text{-}imp}$ represents the MZW in the presence of crystal seeds or impurity ions.

2.4. Chemical and physical characteristics of three tested crystal seeds

Three crystal seeds (Quartzite, Calcite and Dolomite) were prepared by crushing, rinsing, air-drying and sieving. Particle-size distribution was determined by screening filter with the aperture of 0.15~0.20 mm. The specific surface area of the seeds was measured using multipoint Brunauer–Emmett–Teller (BET) method. X-ray fluorescence spectrometer (XRF) was used to quantitatively analyze the components of seeds. The test of specific surface area and constituent content were executed by professional testing company (ZKBaice Co., Ltd., Beijing, China).

3. Results and discussion

3.1. The solubility and metastable zone of HAP

3.1.1. Dissolution characteristics of HAP at different saturation temperatures

The electrical conductivity is related to the ion concentration and species in solution. The ions concentration of solution can be directly reflected by electrical conductivity due to the fact that conductivity is increased with the increase of ionic concentration in the solution [29, 33]. The dissolution characteristics of HAP at different temperatures were investigated by measuring electrical conductivity and pH value at its corresponding temperatures. Fig. 3 shows that the electrical conductivity of solution was increased with the rise of temperature, but the pH value was decreased with the rise of temperature. HAP is a sparingly soluble salt (K_{sp} = 2.35 × 10^{-59} mol/L, 25°C) at room temperature, and its solubility is increased with the rise of temperature. Meanwhile,

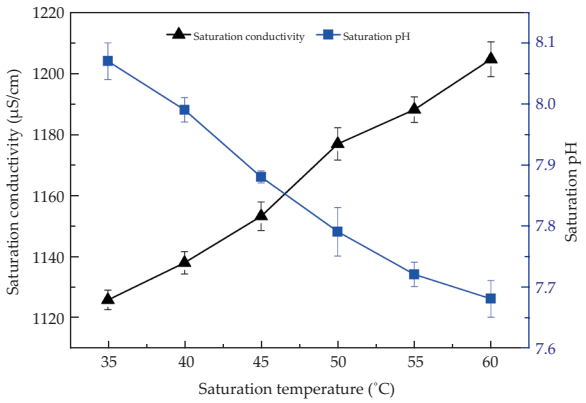

Fig. 3. Electrical conductivity and pH value of HAP solution at different saturation temperatures (200 r/min, heating rate 10°C/h, data points represent the means ± standard of three batch experiments).

the hydroxyl of HAP is more similar to the hydroxyl group in organic matter, and it is easier to release hydrogen ions, thus resulting in the decrease of pH [27].

3.1.2. The effects of different cooling rate for MZW of HAP

The saturated solution at a certain temperature was cooled with the cooling rate of 5~20°C/h. The crystals were formed when the temperature of solution reduced up to a critical value and the electrical conductivity of the solution decreased sharply. Meanwhile, the ions concentration was decreased and the turbidity increased in the solution due to the generated crystallized products. It was owing to the fact that ionic composition of HAP in solution is driven by a certain degree of saturation, and then a new phase particles was formed with no clear boundaries [16]. Most incipient molecular clusters are in an unstable dynamic equilibrium, and some of them continue to grow, while others are split or re-dissolved [20]. The driving force for crystallization is increased with the reduction of temperature, and then the molecular clusters gradually grow to the stable size and establish thermodynamic equilibrium relationship in the solution. By this time, the incipient crystals are no longer disintegration and continue to grow as crystal nucleus [34, 35].

As shown in Fig. 4, the MZW of HAP was increased gradually with the increased cooling rate. Compared with the higher saturation temperature, MZW was smaller at lower saturation temperature at same cooling rate. Recently, a new approach for the theoretical treatment of MZW data was proposed by Kubota [36], which was not considered in Nývlt's approach [20]. This approach accounts for the dependence of the measured MZW's, for a given solution system on the detection technique utilized to indicate the first nucleation events. The Kubota's Eq. (3) showed the relationship between MZW and cooling rate:

$$Log(\Delta T_{max}) = \frac{1}{n+1}\log(R) + \frac{1}{n+1}\log\left[\left(\frac{N_m}{V}\right) - \left(\frac{k_n}{n+1}\right)\right] \quad (3)$$

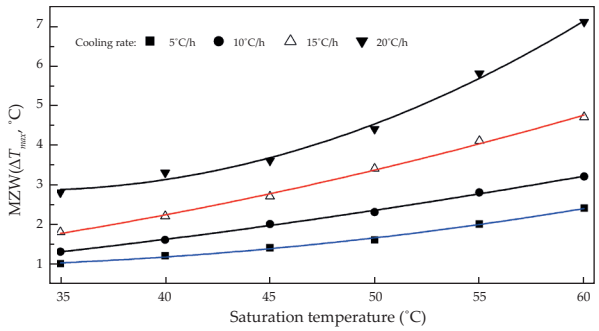

Fig. 4. The effects of different cooling rates on MZW of HAP.

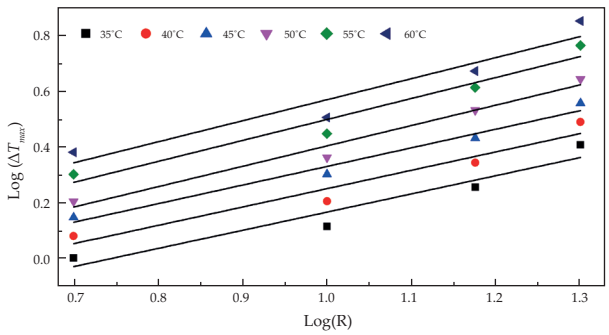

Fig. 5. The relationship between MZW and cooling rate.

where n means the nucleation order, N_m is the accumulated number of grown primary nuclei by the time t, V is the working volume of a crystallizer, and kn is the nucleation constant. This equation can be fitted to a trend line of a log plot of the MZW, Log(ΔT_{max}), versus the cooling rate, log(R), for a given saturation concentration, similar to Nývlt's equation [20]. Eq. (3) predicts a constant slope 1/(n+1) and different intercepts, which correspond to the method of measurement of MZW [36]. The linear relationship between Log(ΔT_{max}) and Log(R) is:

$$Y = AX + B \tag{4}$$

In Eq. (4), $A = \frac{1}{n+1}$, $B = \frac{1}{n+1}\log\left[\left(\frac{N_m}{V}\right) - \frac{1}{n+1}\left(\frac{K_n}{n+1}\right)\right]$, and the nucleation order n can be deduced from the slope of the linear relation between Log(ΔT_{max}) and Log(R). The relationship between the MZW and the cooling rate R at different saturation temperatures is shown in Table 1 and Fig. 5. The Log(ΔT_{max}) and Log(R) in the equation have a linear relation at different saturation temperatures. Theoretically, each line is parallel, and saturation temperature could not affect the nucleation order of solution series. However, Table 1 and Fig. 5 show that the straight line is not absolutely parallel. It might be caused by the experimental errors in the measurement process and could be modified by Eq. (5) [20]:

Table 1
Nucleation equations and parameters of HAP under different saturated temperatures

Saturation temperature (°C)	Nucleation equation	A	B
35	Y = 0.753X + 0.152	0.753	0.152
40	Y = 0.751X + 0.113	0.751	0.113
45	Y = 0.729X + 0.079	0.729	0.079
50	Y = 0.666X + 0.071	0.666	0.071
55	Y = 0.658X + 0.111	0.658	0.111
60	Y = 0.652X + 0.124	0.652	0.124

$$A = \frac{\sum_{j=1}^{p}\left[\sum_i x_i y_i - \sum_i x_i / N_j \times \sum_i y_i\right]_j}{\sum_{j=1}^{p}\left[\sum_i x_i^2 - (\sum_i x_i)^2 / N_j\right]_j} \tag{5}$$

In Eq. (5): x_i = Log(R)$_i$, y_i = Log(ΔT_{max})$_i$, p represents the number of lines, N_j means the number of experiments for each line. The A value was 0.701 by Eq. (5), according to the above results, the nucleation orders of HAP solution was 0.426.

3.2. The effects of crystal seeds and dosage for MZW of HAP

3.2.1. The effects of different crystal seeds for MZW

In induced crystallization reaction, the presence of crystal seeds can decrease the interfacial energy of crystallization reaction and make the crystal precipitate on the seeds surface easy [19, 20]. Several studies indicated that the effects on induced crystallization efficiency were related to the characteristics of the seeds. The chemical composition of seeds is similar to the crystal and has a higher specific surface area, which are beneficial to the crystallization reaction [22]. A study by Ashok et al. [37] showed that calcium had a positive effect on the crystallization efficiency. Therefore, the chemical and physical characteristics of the three kinds of seeds had been analyzed in this study, and the results are shown in Table 2. In comparison with dolomite seeds, calcite seeds had a lower density of 2.86 g/cm^3, leading to an increase of internal porosity and a larger surface area of reaction. Quartzite, containing trace of calcium (2.8%, Table 2), showed a lower density of 2.65 g/cm^3 than calcite, but its specific surface area was lower than calcite. Dolomite seed was composed of calcium and magnesium, having the potential to promote struvite formation. The density (3.05 g/cm^3) of dolomite was the highest among three tested seeds, which resulted in a lower specific surface area of 0.0107 m^2/g. Fig. 6 shows that the presence of crystal seeds could increase the width of the metastable zone. Consequently, calcite seed exhibited the best performance on the improvement of MZW and was employed as the crystal seed in the following induced crystallization reactions.

Table 2
Chemical and physical characteristics of the three tested media

Material	Chemical composition (% W/W)					Density (g/cm^3)	Specif. area (m^2/g)	Particle size (mm)
	Ca	Si	Mg	Fe	Al			
Quartzite	2.80	74.46	–	5.02	0.91	2.65	0.0347	0.15–0.20
Dolomite	86.43	0.32	10.57	2.16	0.20	3.05	0.0107	0.15–0.20
Calcite	98.21	0.15	0.01	0.33	0.12	2.86	0.0746	0.15–0.20

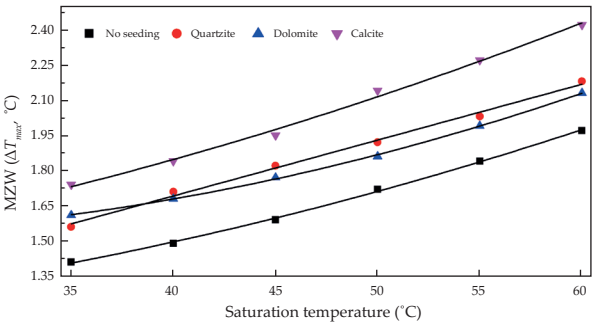

Fig. 6. The effects of different crystal seeds on MZW.

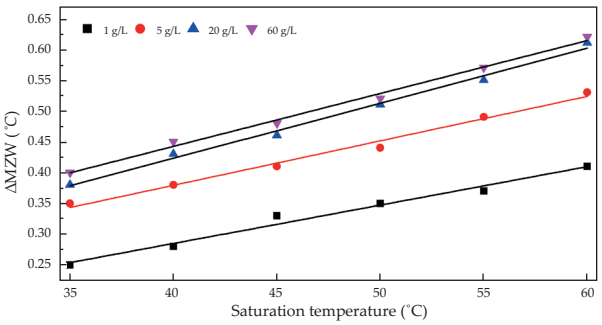

Fig. 7. The effects of seeds dosage on MZW.

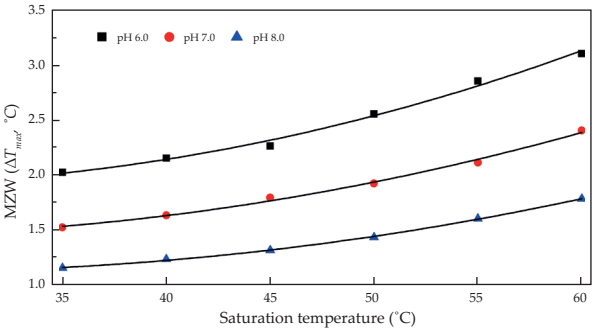

Fig. 8. The effects of initial pH of solution on MZW.

3.2.2. The effects of seeds dosage on MZW

The effects of seeds dosage (Calcite) on MZW was obtained at the initial pH 7.0, 200 r/min, and cooling rate 10°C/h. As can be seen in Fig. 7, the variation of MZW was increased gradually with the increase of the crystal seeds dosage. The variation amplitude was increased with the rise of saturation temperature. Meanwhile, the increased amplitude of the MZW with the addition of seed crystal at 20 g/L was similar to the addition of 60 g/L. Our rationalization for this behavior is that the existence of the crystal seeds can reduce the energy barrier in the process of crystallization to induce the nucleation formation [20]. The increased addition of crystal seeds would consume the saturation degree of HAP solution and enlarge the width of the metastable zone [16]. However, MZW of HAP crystallization could not be increased when the amount of crystal seeds reached to some extent. Therefore, the dosage of crystal seeds should be controlled in the appropriate range in inducing crystallization process.

3.3. The effects of initial pH of solution on MZW

The solubility of HAP in aqueous solution was influenced by pH, temperature, over saturation of constituents, etc. pH can greatly affect the dissolution of HAP. In acidic solution, HAP can produce PO_4^{3-}, $CaOH^+$, $CaPO_4^-$, $H_2PO_4^-$, Ca^{2+}, etc. in which the following reaction may occur [28]:

$$Ca_5(PO_4)_3OH + H^+ = 5Ca^{2+} + 3PO_4^{3-} + H_2O \quad (6)$$

$$Ca_5(PO_4)_3OH + 4H^+ = 5Ca^{2+} + 3HPO_4^{2-} + H_2O \quad (7)$$

$$Ca_5(PO_4)_3OH + 7H^+ = 5Ca^{2+} + 3H_2PO_4^- + H_2O \quad (8)$$

This section investigated the effects of initial pH on MZW at 200 r/min, cooling rate of 10°C/h and calcite as seeds (5g/L). The initial pH value was 6, 7 and 8 at saturation temperature of 60°C, and corresponding electrical conductivity was 1,434.9, 1,318.3, 1,204.6, respectively (data not shown). As can be seen in Fig. 8, acidic solution (pH 6.0) had a larger MZW than alkaline solution (pH 8.0). It is due to the fact that H^+ in acidic solution can improve the dissolution of HAP [28], delaying the critical saturation point occurrence, and leading to the increase of MZW.

3.4. The effects of stirring intensity on MZW

Classical nucleation theory holds that higher mixing intensity can promote the probability of collision nucleation and increase the energy distribution timely in process of crystallization. Meanwhile, it can also take the occurrence

time of nucleation in advance and narrow the MZW [20]. The effects of stirring intensity (100, 200, 300, 400 and 500 r/min) on MZW variation was investigated at the initial pH 7.0, a cooling rate of 10°C /h, and calcite as seeds (5 g/L). At the same saturation temperature, the larger stirring intensity resulted in a narrower MZW (Fig. 9), which indicated that the higher flow velocity can shorten the nucleation time. The effect of the stirring intensity on MZW was gradually weakened with the decreased of saturation temperature. The ions, adsorbing on the seeds before their nucleation, would be washed away with a high stirring rate thus inhibiting the formation of crystal nucleus [16, 20]. Therefore, appropriate stirring intensity is indispensible for HAP induced crystallization.

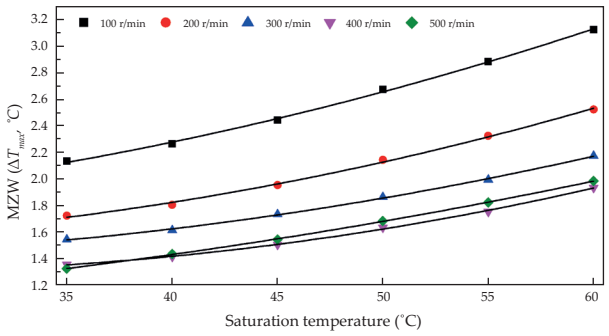

Fig. 9. The effects of stirring intensity on MZW.

3.5. MZW variation in the presence of typical impurity ions

The presence of impurities in the solution has an important impact on the MZW of a solid-solvent system. Recently, several studies have investigated the solubility and MZW of phosphoric acid in the presence of cationic and anionic impurities, and the results showed that they can increase the MZW [38–40]. However, the effects of impurity ions on the MZW of the sparingly soluble HAP solution have been rarely reported. Fig. 10 presents plots of four impurity ions and their dosage against ΔMZW for HAP solutions at 200 r/min, and calcite as seeds (5 g/L).

It is found that the A, B, C, and D showed the similar trends at various saturation temperatures, respectively (Fig. 10). The linear plots represented the best fit of the experimental data. The four kinds of impurity ions were all capable of increasing the MZW of HAP, and ΔMZW was increased with the rise of impurity ion concentration. In the high saturation temperature region, the effect of four impurity ions was obviously enhanced. The biggest variation of ΔMZW was 1.81°C in the presence of CO_3^{2-}, and the smallest variation was 1.17°C with SO_4^{2-}. The effect of CO_3^{2-} on ΔMZW in the high saturation temperature (60°C) was a 1.5-fold increase than that in the low saturation temperature (35°C). It is generally believed that the impurity ions are adsorbed on the crystal surface, resulting in the increase of the energy level for the precipitation of crystal products, and enlarging the energy barrier of crystallization [41]. Compared with the condition of no impurity ions, the nucleation in

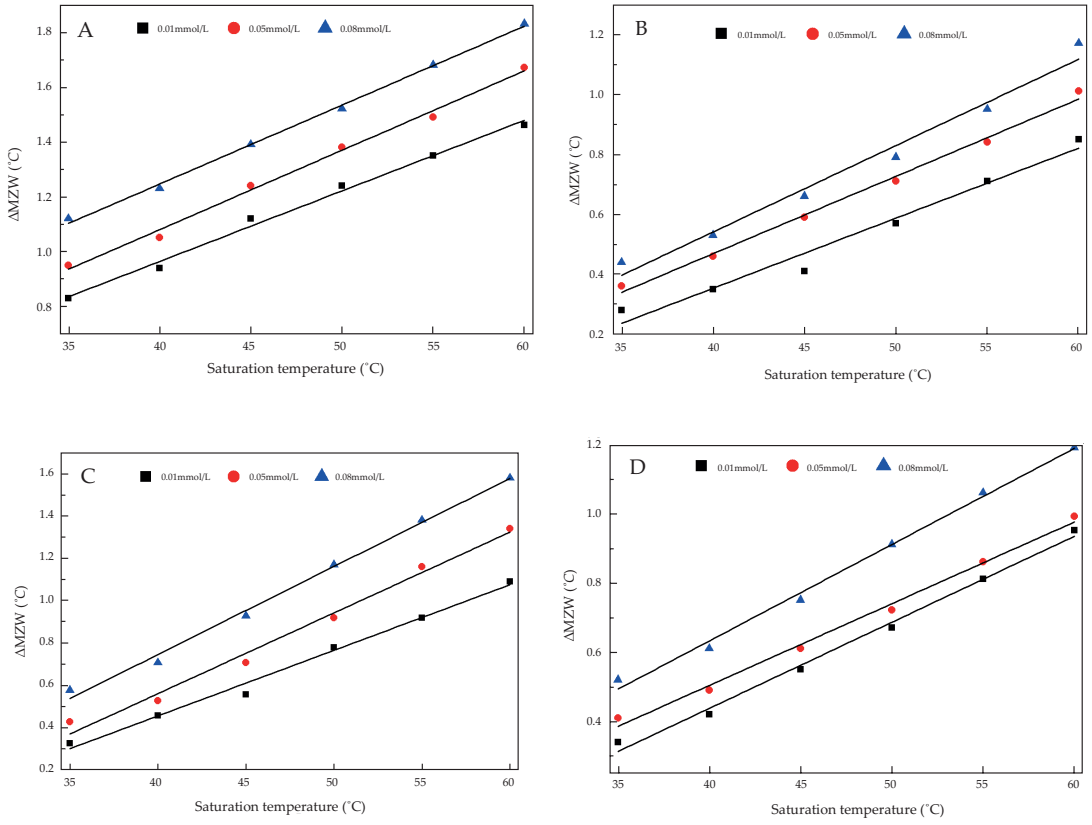

Fig. 10. The variation of MZW in the presence of typical impurity ions (A: CO_3^{2-}, B: SO_4^{2-}, C: Fe^{3+}, D: Cu^{2+}).

the crystallization process requires a greater impetus. The higher energy barrier needs to overcome the crystal growth in the high concentration of impurity ions. Fig. 10 shows the effect of four impurity ions on the metastable zone of HAP, and the orders was: $CO_3^{2-} > Fe^{3+} > Cu^{2+} > SO_4^{2-}$.

4. Conclusions

The metastable zone of solution is the precondition of HAP crystallization reaction. In order to explore the characteristics of metastable zone of sparingly soluble HAP, a method using electrical conductivity and turbidity was developed. Several experimental factors (crystal seeds, initial pH, agitation level, impurities) were also investigated to illuminate the effects on the MZW of HAP crystallization:

(a) In the range of saturation temperature (35~60°C), MZW of HAP was increased with the increase of cooling rate. According to Kubota's equation, the Log(ΔT_{max}) and Log(R) had a linear relationship, and the apparent nucleation progression of HAP was 0.426.
(b) The presence of crystal seeds consumed the degree of solution saturation, thus expanding MZW of HAP. Among the three crystal seeds (Dolomite, Quartzite and Calcite), the calcite exhibited the best performance on improving the MZW due to its characteristics.
(c) The larger stirring intensity resulted in a narrower MZW indicated that the higher flow velocity could shorten the nucleation time. Acidic solution (pH 6.0) had a larger MZW than the solution with pH 8.0.
(d) All kinds of impurity ions could increase the MZW of HAP. The biggest variation of MZW was 1.81°C in the presence of CO_3^{2-}, and the smallest variation was 1.17°C with SO_4^{2-}. The order of the impact of impurity ions on ΔMZW was: $CO_3^{2-} > Fe^{3+} > Cu^{2+} > SO_4^{2-}$.

Acknowledgement

This work was supported by the National Twelfth Five-Year Major Projects (2012ZX07101-005), the National Natural Science Foundation of China (51078074), the Scientific Research Foundation of Graduate School of Southeast University, and the Research Innovation Program for College Graduates of Jiangsu Province (KYLX15_0073). The authors wish to thank the anonymous reviewers for their constructive comments that improved the manuscript.

References

[1] W. Guan, F.Y. Ji, Q.K. Chen, P. Yan, Q. Zhang, Preparation and phosphorus recovery performance of porous calcium-silicate-hydrate, Ceram. Int., 39 (2013) 1385–1391.
[2] M.M. Rahman, M.A.M. Salleh, U. Rashid, A. Ahsan, M.M. Hossain, C.S. Ra, Production of slow release crystal fertilizer from wastewaters through struvite crystallization—A review, Arab. J. Chem., 7 (2014) 139–155.
[3] K.S. Le Corre, E. Valsami-Jones, P. Hobbs, S.A. Parsons, Phosphorus Recovery from Wastewater by Struvite Crystallization: A Review, Crit. Rev. Env. Sci. Tec., 39 (2009) 433–477.
[4] C. Fang, T. Zhang, P. Li, R.F. Jiang, S.B. Wu, H.Y. Nie, Y.C. Wang, Phosphorus recovery from biogas fermentation liquid by Ca-Mg loaded biochar, J. Environ. Sci., 29 (2015) 106–114.
[5] L. Qiu, P. Zheng, M. Zhang, X. Yu, G. Abbas, Phosphorus removal using ferric–calcium complex as precipitant: Parameters optimization and phosphorus-recycling potential, Chem. Eng. J., 268 (2015) 230–235.
[6] Z.L. Ye, S.H. Chen, S.M. Wang, L.F. Lin, Y.J. Yan, Z.J. Zhang, J.S. Chen, Phosphorus recovery from synthetic swine wastewater by chemical precipitation using response surface methodology, J. Hazard. Mater., 176 (2010) 1083–1088.
[7] J.S. An, Y.J. Back, K.C. Kim, R. Cha, T.Y. Jeong, H.K. Chung, Optimization for the removal of orthophosphate from aqueous solution by chemical precipitation using ferrous chloride, Environ. Technol., 35 (2014) 1668–1675.
[8] A. Oehmen, P.C. Lemos, G. Carvalho, Z. Yuan, J. Keller, L.L. Blackall, M.A. Reis, Advances in enhanced biological phosphorus removal: from micro to macro scale, Water Res., 41 (2007) 2271–2300.
[9] M. Li, Y. Wu, Z. Yu, G. Sheng, H. Yu, Enhanced nitrogen and phosphorus removal from eutrophic lake water by *Ipomoea aquatica* with low-energy ion implantation, Water Res., 43 (2009) 1247–12456.
[10] C. dos Santos, A. Ribeiro, M.R. Teixeira, Phosphorus recovery from waters using nanofiltration, Desalin. Water Treat., 55 (2015) 1308–1315.
[11] J. Altmann, A. Sperlich, M. Jekel, Integrating organic micropollutant removal into tertiary filtration: Combining PAC adsorption with advanced phosphorus removal, Water Res., 84 (2015) 58–65.
[12] J. Shi, X. Lu, R. Yu, W. Zhu, Nutrient removal and phosphorus recovery performances of a novel anaerobic-anoxic/nitrifying/induced crystallization process, Bioresour. Technol., 121 (2012) 183–189.
[13] M. Hanhoun, L. Montastruc, C. Azzaro-Pantel, B. Biscans, M. Frèche, L. Pibouleau, Simultaneous determination of nucleation and crystal growth kinetics of struvite using a thermodynamic modeling approach, Chem. Eng. J., 215–216 (2013) 903–912.
[14] Y. Shen, Z. Ye, X. Ye, J. Wu, S. Chen, Phosphorus recovery from swine wastewater by struvite precipitation: compositions and heavy metals in the precipitates, Desalin. Water Treat., (2015) 1–9.
[15] K. Sangwal, Recent developments in understanding of the metastable zone width of different solute-solvent systems, J. Cryst. Growth, 318 (2011) 103–109.
[16] S.A. Kulkarni, S.S. Kadam, H. Meekes, A.I. Stankiewicz, J.H. Horst, Crystal Nucleation Kinetics from Induction Times and Metastable Zone Widths, Cryst. Growth Des., 13 (2013) 2435–2440.
[17] S.S. Kadam, S.A. Kulkarni, R. Coloma Ribera, A.I. Stankiewicz, J.H. Horst, H.J.M. Kramer, A new view on the metastable zone width during cooling crystallization, Chem. Eng. Sci., 72 (2012) 10–19.
[18] D.C. Huang, W. Liu, S.K. Zhao, Y.Q. Shi, Z.X. Wang, Y.M. Sun, Quantitative design of seed load for solution cooling crystallization based on kinetic analysis, Chem. Eng. J., 156 (2010) 360–365.
[19] J. Nývlt, The effect of the cooling method on the crystal size distribution of the product from a batch crystallizer, Coll. Czech. Chem. C., 39 (1974) 3463–3472.
[20] J. Nývlt, O. Sohnel, M. Matuchova, M. Broul, In: *The Kinetics of Industrial Crystallization*, Academia, Prague, 1985.
[21] H. Li, Z. Guo, B. Xue, Y. Zhang, W. Huang, Collagen modulating crystallization of apatite in a biomimetic gel system, Ceram. Int., 37 (2011) 2305–2310.
[22] N. Bellier, F. Chazarenc, Y. Comeau, Phosphorus removal from wastewater by mineral apatite, Water Res., 40 (2006) 2965–2971.
[23] Y. Song, P.G. Weidler, U. Berg, R. Nuesch, D. Donnert, Calcite-seeded crystallization of calcium phosphate for phosphorus recovery, Chemosphere, 63 (2006) 236–243.
[24] E.H. Kim, H.K. Hwang, S.B. Yim, Phosphorus removal characteristics in hydroxyapatite crystallization using converter slag, J. Environ. Sci. Heal. A., 41 (2006) 2531–2545.
[25] P. Battistoni, P. Pavan, F. Cecchi, J. Mata-Alvarez, Phosphate removal in real anaerobic supernatants: Modelling and performance of a fluidized bed reactor, Water Sci. Technol., 38 (1998) 275–283.

[26] M.M. Seckler, O.S.L. Bruinsma, G.M. VanRosmalen, Calcium phosphate precipitation in a fluidized bed in relation to process conditions: A black box approach, Water Res., 30 (1996) 1677–1685.
[27] M.T. Fulmer, I.C. Ison, C.R. Hankermayer, B.R. Constantz, J. Ross, Measurements of the solubilities and dissolution rates of several hydroxyapatites, Biomaterials, 23 (2002) 751–755.
[28] H.B. Pan, B.W. Darvell, Solubility of hydroxyapatite by solid titration at pH 3-4, Arch. Oral. Biol., 52 (2007) 618–624.
[29] L.F.E. Nathalie, O. Louisnard, S. Jacques, Effect of ultrasound on the induction time and the metastable zone widths of potassium sulphate, Chem. Eng. J., 86 (2002) 233–241.
[30] K.J. Kim, A. Mersmann, Estimation of metastable zone width in different nucleation processes, Chem. Eng. Sci., 56 (2001) 2315–2324.
[31] J. Ulrich, C. Strege, Some aspects of the importance of metastable zone width and nucleation in industrial crystallizers, J. Cryst. Growth, (2002) 237–239.
[32] X. Zhang, Z. Yang, J. Chai, J. Xu, L. Zhang, G. Qian, X. Zhou, Nucleation kinetics of lovastatin in different solvents from metastable zone widths, Chem. Eng. Sci., 133 (2015) 62–69.
[33] L. Dang, H. Wei, Z. Zhu, J. Wang, The influence of impurities on phosphoric acid hemihydrate crystallization, J. Cryst. Growth, 307 (2007) 104–111.
[34] J. Nývlt, R. Rychlý, J. Gottfried, J. Wurzelová, Metastable zone-width of some aqueous solutions, J. Cryst. Growth, 6 (1970) 151–162.
[35] Z.K. Nagy, M. Fujiwara, X.Y. Woo, R.D. Braatz, Determination of the kinetic parameters for the crystallization of paracetamol from water using metastable zone width experiments, Ind. Eng. Chem. Res., 47 (2008) 1245–1252.
[36] N. Kubota, A new interpretation of metastable zone widths measured for unseeded solutions, J. Cryst. Growth, 310 (2008) 629–634.
[37] M. Ashok, N. Meenakshi Sundaram, S. Narayana Kalkura, Crystallization of hydroxyapatite at physiological temperature, Mater. Lett., 57 (2003) 2066–2070.
[38] L.P. Dang, Z.Z. Wang, P.B. Liu, Measurement of the metastable zone width of phosphoric acid hemihydrate in the presence of impurity ions, J. Chem. Eng. Data., 52 (2007) 1545–1547.
[39] Y. Ma, J. Zhu, H. Ren, K. Chen, Effects of impurity ions on solubility and metastable zone width of phosphoric acid, Cryst. Res. Technol., 44 (2009) 1313–1318.
[40] K. Sangwal, On the effect of impurities on the metastable zone width of phosphoric acid, J. Cryst. Growth, 321(2010) 3316–3325.
[41] K. Sangwal, E. Mielniczek-Brzóska, Effect of impurities on metastable zone width for the growth of ammonium oxalate monohydrate crystals from aqueous solutions, J. Cryst. Growth, 267 (2004) 662–675.